

**THESIS: Three Experimental Tests of
Bell's Inequalities ...**

*(Trois tests expérimentaux des
inégalités de Bell)*

*Alain Aspect, Université Paris-Sud,
PhD thesis no. 2674*

CHAPTER VI, SECTION C

Detection and Counting of Coincidences

Translated, March 1996

Caroline H Thompson
Department of Computer Science
UW Aberystwyth
Dyfed, SY23 3DB

e-mail: cat@aber.ac.uk

April 10, 1997

VI-C Detection and Counting of Coincidences

[- 212 -]

VI-C-1 Overview of the system

Fig. VI-11 shows the organisation of the coincidence counting system for two photomultipliers*.

The anode pulses from the photomultipliers, associated with the detection of photons, are shaped by the discriminators. Part of each is counted directly (singles counts), and the other part sent to the two coincidence counting systems.

The progress of the experiment is governed by a clock that authorises the accumulation of data during pre-selected periods (usually 100 s).

At the end of each period, the values obtained can be transferred to a mini-computer that stores them on floppy disk, accompanied by relevant parameter values (orientations of the polarisers, duration of accumulation period etc. ...).

It is then easy, at the end of a cycle of measurements, to analyse the data using the same computer.

Remark: *We used standard electronic N.I.M (Nuclear Instrument Module) modules, that offered great flexibility for constructing the desired configuration. Unfortunately, this standard was not geared towards control by computer (in contrast to the more recent and expensive standard C.A.M.A.C.). We therefore had to construct complicated interfaces between the N.I.M. modules and the computers.*

[- 213 -]

*The system for four photomultipliers, which is more complicated but uses the same principles, can be seen in Chapter VIII.

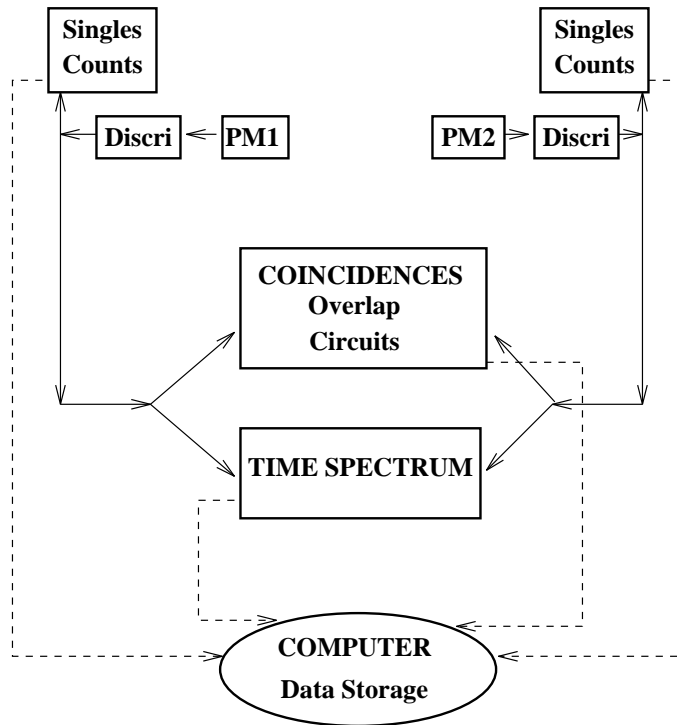


Figure VI-11: Organisation of the detection and coincidence counting systems.

In the detailed description of the system, we use typical orders of magnitude. We refer to an experiment in which the source functions in the optimal regime; that is to say, it emits

$$N = 4 \times 10^7 \text{ pairs/s}$$

[- 214 -]

We shall take typical global detection efficiencies

$$\varepsilon_1 = \varepsilon_2 = 2 \times 10^{-3}$$

The counts, in the absence of polarisers, would then be (cf. § V-1):

- Singles counts:

$$N_1 = N_2 = \varepsilon N = 8 \times 10^4 \text{ s}^{-1}$$

- True coincidences (*coïncidences vrais*):

$$N_v = P\varepsilon_1\varepsilon_2N \cong 200 \text{ s}^{-1} \quad (\text{VI} - 6)$$

- Accidental coincidences (*coïncidences fortuites*):

$$\frac{dN_f}{d\tau} = N_1N_2 = 6.4 \times 10^9 \text{ s}^{-2},$$

(that is to say 64 s^{-1} for a window of 10 ns)

VI-C-2 Detection. The photomultiplier-discriminator ensemble

a) Principles

The principles of photon counting have been known for a long time⁽¹²⁰⁾. When an electron is emitted from the photocathode, it is accelerated

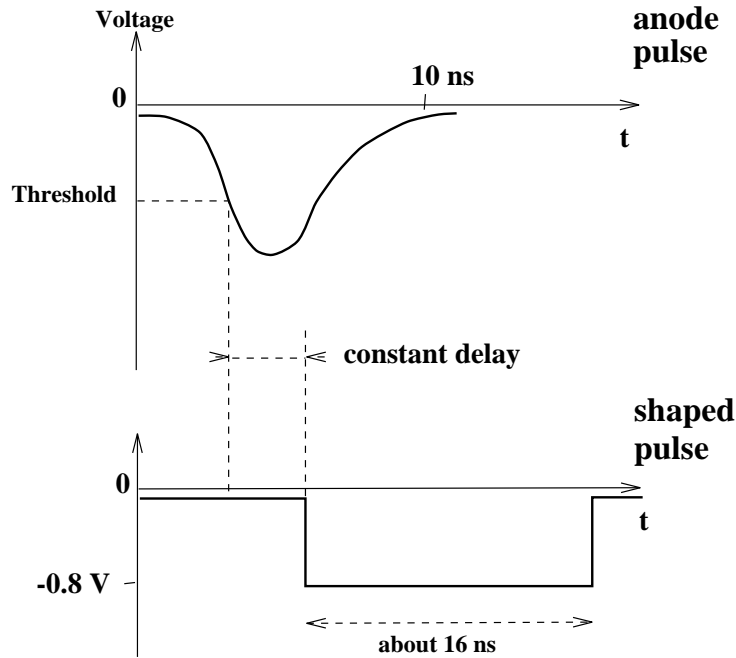


Figure VI-12: Shaping of the anode pulse by the discriminator.

towards the first dynode of the photomultiplier. The impact causes the emission of a secondary shower of electrons. The process continues in a cascade from dynode to dynode, and produces a brief pulse of current at the anode.

For a typical gain of 3×10^7 , the charge of each anode pulse is 5×10^{-12} Coulomb, delivered in a few nanoseconds. A voltage of a few tens of millivolts is obtained across a resistance of 50 Ohms.

[- 215 -]

Remark: *All the high frequency circuits are connected by coaxial cables terminated by resistors of 50Ω , equal to their characteristic impedances. This avoids reflections that would give “parasitic” pulses, causing multiple outputs.*

As the process of multiplication is stochastic (deriving from Poisson processes), the anode pulses show great variations in shape and am-

plitude. It is necessary to convert them to a standard form, which is done with the aid of the discriminator, a thresholding system that delivers a pulse that rises abruptly whenever the anode pulse exceeds the threshold (Fig. VI-12).

[- 216 -]

The transition $0 V \rightarrow -0.8 V$ takes place at an instant that is well defined with respect to the time at which the threshold is exceeded. It is this transition to which the N.I.M. circuits, situated after the discriminator, are sensitive.

b) Discriminator threshold

The choice of threshold value for the discriminator is a delicate problem. Once the voltage of the photomultiplier has been fixed, the efficiency of detection increases as the threshold is lowered, as one detects smaller anode pulses.

But, at the same time, the discriminator becomes sensitive to a greater number of parasitic pulses, not corresponding to a photoelectron. These parasitic pulses (dark counts) have many causes: thermal emission of electrons from the cathode, or from the first dynode; internally induced discharges due to residual ions, externally induced discharges between electrodes.

Despite the abundance of literature on the question of choice of threshold^(120,135,136), we think there is no “universal recipe”. One must look at the characteristic curves for the particular tube used, and deduce from them the best choice for the precise problem under consideration.

Fig. VI-13 shows the curves obtained for one of our photomultipliers. The frequency of detections is shown, for fixed photomultiplier voltage and constant incident light flux, as a function of the threshold. Also shown is the curve for the dark count, obtained with zero incident light.

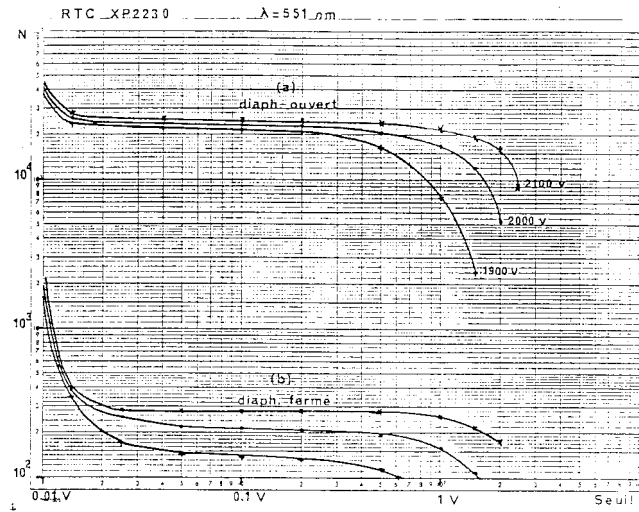


Figure VI-13: Singles counts as function of discriminator threshold, for various values of photomultiplier voltage.
 (a) Photocathode illuminated by light at 551 nm
 (b) Dark count

The curves obtained show (on a logarithmic scale) a definite plateau. This is interpreted as indicating that the electrons emitted by the photocathode produce pulses with amplitudes that are not too variable. So long as the value of the threshold is definitely smaller than these amplitudes, one is in the plateau.

[- 218 -]

For the dark counts, the plateau corresponds to events happening at the photocathode (thermal emissions), whilst the increase at low amplitude is due to parasitic phenomena at intermediate dynodes, which are amplified less.

It is advisable in general to work within the plateau, in order to discriminate well between true and parasitic counts. But, in truth, the plateau is not perfectly horizontal; the frequency of true counts (total

number less dark counts) grows as the threshold decreases, so that the *effective efficiency of photon counting* increases.

When the system must be pushed to its limits, the criteria for regulating it must be taken from a study of the ratio of signal to noise. In a photon counting experiment, the noise is not the dark count (which is easy to subtract from the total signal), but the Poissonian variations of the total signal. The signal to noise ratio behaves differently according as the true signal is large or small compared to the dark count, and each situation must be studied separately. These considerations lead most often to choosing a very low threshold, at the extreme left of the plateau: although the dark count is stronger here, one finds in general a better signal to noise ratio.

Under these conditions, problems with instabilities or with system drift can be encountered. For exact measurements, therefore, it is better to remain in a more central part of the plateau, at the expense of slightly reducing the effective efficiency.

[- 219 -]

One rule can be made: if there is evidence that a presumed signal is weak, it is advantageous to choose a very low threshold, giving the best detection efficiency; but if precise measurements must be made, necessitating a constant efficiency, it is better to choose a higher threshold, within a more horizontal part of the plateau.

The preceding discussion relates to singles counts. In an experiment involving coincidences, the dark count is no problem if it does not give rise to an excessive number of accidental coincidences. This is the case if the dark rate is small compared to the singles rate. As the signal to noise ratio increases with the detection efficiency (§V-1), there is reason to use a low threshold.

But if reproducibility of measurements is more important, it is preferable to sacrifice a little sensitivity and choose the centre of the plateau. This is the choice we have made.

c) Photomultiplier high tension

Increased high tension gives a number of advantages. The plateau is more marked when the voltage is high (Fig. VI-13), and the detection efficiency is increased. A high discriminator threshold can be used, avoiding the need for an amplifier between the photomultiplier and discriminator. Moreover, a high voltage improves the temporal resolution of the system (cf. § d below).

Unfortunately, though, there is at the same time an increase in the probability of occurrence of certain instabilities in the tube, particularly in the configuration used for photon counting. In this configuration, the anode is neutral (potential near earth) and the enclosing glass tube is, like the cathode, at a large negative potential (-2000 Volts to -3000 Volts). There are sometimes violent parasitical discharges, rendering the system useless.

[- 220 -]

An effective precaution consists of cleaning the tube very well, and enveloping it in teflon foil before inserting it in its shielding container. In addition, the voltage should be increased by small stages from 1500 Volts onwards. It is necessary to keep the dark counts permanently under control: at each new level of the voltage, this count, starting high, should decrease steadily. At the least sign of increase of the count (for a fixed voltage), the voltage must immediately be reduced, for there is the risk of an explosion. When the desired regime is attained, it is best to leave the photomultiplier powered up. Experience shows that the dark counts can continue to decrease over more than 24 hours.

Given these precautions, it is possible to attain the highest voltages authorised by the manufacturers (between 2500 V and 3000 V). A return to a slightly lower value enables functioning without risk of incident.

d) Temporal resolution

There is a delay separating the emission of a primary electron at the photocathode and the front of the N.I.M. pulse being delivered by the discriminator. This delay, of the order of 30 ns, can vary, and it is this that limits the resolution of time measurements.

We have measured, with the aid of a sampling oscilloscope, the fluctuations due to the discriminator alone: they are less than 0.1 ns.

[- 221 -]

By contrast, the transit time in the photomultiplier (of the order of 30 ns) is subject to larger fluctuations, due to the statistical nature of the amplification process, and to “*l'écart centre-bord*” (variation between photoelectrons emitted at centre and border of the photocathode).

These variations are usually represented⁽¹²⁰⁾ by describing the distribution of transit times by a gaussian, for which one gives the standard error. We were not able to measure the variance directly, as we had no source that emitted sufficiently short pulses.

Nevertheless, we evaluated the overall temporal resolution of our system of coincidences from the time spectrum, by measuring the rise time of the spectrum associated with our atomic cascade (cf. § VI-C-3). This rise time is of the order of 2 ns between 16% and 84%, and a gaussian of standard error about 1 ns can be associated with it.

If we assume the two photomultipliers are identical, it follows that a gaussian of standard error 0.7 ns can be attributed to each, which compares well with the manufacturer's specification: 0.35 ns variation in the transit time of electrons emitted at the centre of the photocathode, and 0.6 ns variation between centre and border.

The temporal resolution can be improved by increasing the voltage applied to the photomultiplier tubes: the transit time decreases as

$U^{-1/2}$. One cannot, however, proceed far in this direction.

Remark 1: *Nuclear physicists assert that they achieve resolutions today of 0.1 ns, which might seem to contradict our results. The difference is that they work with intense pulses (associated with the passage of a particle in a scintillator). The shower of electrons corresponding to a light pulse leads to an anode pulse of great amplitude, for which the centre of gravity is well defined as a result of the statistical properties of the mean. By contrast, in our case, a single electron is emitted each time.*

[- 222 -]

Remark 2: *In nuclear physics, the time resolution is improved by using “constant fraction discriminators”, for which the threshold is a function of the maximum amplitude received. This avoids variations in delay linked to variations in pulse amplitudes (cf. Fig. VI-12). We have tried these same discriminators, but found no noticeable improvement. The strength of our pulses is not sufficiently great to be relevant.*

e) Choice of arrangement of photomultipliers

We chose for the two wavelengths photomultipliers with photocathodes of trialcaline of type D. The nominal efficiencies are 25% at 422 nm and 6% at 551 nm.

It might seem more judicious to use a photocathode T at 551 nm (nominal efficiency 10%). In fact, the efficiency of a photomultiplier for photon counting is always less than the efficiency of the photocathode. It includes the collection efficiency of the first dynode (which can be as low as 50%), and the efficiency of thresholding by the discriminator.

On the other hand, within one series of photomultipliers considerable variations can be found in mean performance. We tried various tubes, and found examples of photocathodes of type D that were better, at 551 nm, than those of type T (in our conditions of use, and judged by

[- 223 -]

our criteria).

In the event, we used four photomultipliers of photocathode type D (56 DVP, XP 2230 and XP 2232 of RTC).

Each photomultiplier is mounted in a shielding container R.T.C. S 563, composed of two layers. The first, of steel, screens against parasitic electromagnetic waves and cosmic rays. The second, of mu-metal, protects the tube from magnetic fields that could perturb the opto-electronics between the dynodes.

The base of the container carries a printed circuit on which the resistors and capacitors of the dividing bridge are mounted directly. This compact arrangement does not degrade the speed of the tube.

The anode is connected by a terminated coaxial cable (50Ω) to the discriminator input. There is in principle no need for amplification, unless the distance between the photomultiplier and discriminator is more than 10 metres.

In our conditions, the dark rate is always less than 300 s^{-1} . These values are much less than the singles rates (more than 10^4 s^{-1}) and it is therefore unnecessary to cool the photomultipliers.

The detection efficiencies could be measured by the method described in § VI-D-1. They depend on the conditions of use (voltage, threshold), but they are always noticeably less than the cathode efficiencies* (less than 10% for 422 nm, and less than 3% for 551 nm).

[- 224 -]

*This is at first sight surprising, but it has been observed previously by Clauser et al. and also by Fry et al. (private communications). It is essentially attributable to the poor efficiencies of collection of the optical electronics. It is in general not well known to users who have no means of making absolute measurements.

f) The problem of secondary pulses “*post-impulsions*”

There exists, in the technique of photon counting, a phenomenon of parasitic signals that is not fully understood: this concerns “post-impulsions”, secondary pulses that follow the pulse associated with a photoelectron, with a random delay that can be as much as a microsecond.

When working with a low threshold, these secondary pulses are liable to trigger the discriminators, thus augmenting the singles counts. The error can attain several percent.

In augmenting slightly the singles counts, the secondary pulses will also augment the accidental coincidences. In contrast, they have no effect on the true counts.

We have experimental procedures for measuring accidental coincidences and subtracting them from the total: the true coincidence count thus determined is in no way affected by these secondary pulses.

g) Conclusion

The regulation of the photomultiplier-discriminator ensemble involves a compromise between obtaining efficiency of detection as great as possible and good stability, permitting perfectly reproducible measurements.

The temporal resolution is fundamentally limited, when counting single photons, by variations in transit time of the photomultipliers. The limit of resolution (1.4 ns for each photomultiplier) is not negligible compared to the lifetime of the intermediate stage of the cascade (5 ns), and there is a slight smoothing effect on the coincidence time-spectrum.

The total number of true coincidences is not affected by this limited resolution, but the peak is a little broadened. An integration window

must therefore be chosen of sufficient size (cf. § V-2) to include all the true coincidences.

VI-C-3 Coincidences by Time-Spectrum (Fig. VI-14)

a) Time to Amplitude Converter

We have already introduced in § V-1 the time-spectrum of the coincidences: it is the distribution of the detected pairs, as a function of the time interval between the detections of the two members of the pair. The system giving this time spectrum is based on a Time to Amplitude Converter (*Convertisseur Temps-Amplitude (C.T.A.)*) of Start/Stop circuit type.

A pulse applied to the Start opens a window of 100 ns. If, during this window, a pulse is received at the Stop, the system delivers an analogue pulse, between 0 and 5 volts, of height proportional to the interval between the Start and Stop times, with a resolution of 0.1 ns. The height of this pulse is encoded by a 10-bit analogue-to-digital converter.

b) Multichannel analyser

[- 226 -]

The numerical value of the Start-Stop interval is processed by a multichannel analyser that we constructed using a logic board (A.R.I.A.M. board) with an 8080 microprocessor controlling the output devices.

The A.R.I.A.M. board carries 1024 memory locations*. When each number is presented, the contents of the corresponding location are

*There are in fact four identical memory zones, each of 1024 address locations, which permits the simultaneous registration of four time-spectra.

incremented by unity.

The contents of the 1024 memory locations of the A.R.I.A.M. thus represent the histogram:

$$N_c(i) = \int_{i\Delta t}^{(i+1)\Delta t} \frac{dN_c}{d\tau} d\tau \quad (i = 0, 1 \dots 1023).$$

$N_c(i)$ is the number of coincidences detected with a Start-Stop interval between $i\Delta t$ and $(i+1)\Delta t$. It is thus the step function associated with the function $\frac{dN_c(\tau)}{d\tau}$ of § V-1.

The size of the elementary steps of the histogram is

$$\Delta t \cong 0.1 \text{ ns}$$

The 8080 microprocessor, suitably programmed, enables a continuous representation on a graphics terminal of the histograms associated with the contents of the A.R.I.A.M. Both the vertical scale (number of pairs) and the horizontal one (delay) can be varied at any moment, as well as the choice of which portion of the histogram to display.

When the data acquisition is finished, the microprocessor organises its output: it copies the histograms that have been displayed to the printer, and transfers the contents of the A.R.I.A.M. to the central computer.

[- 227 -]

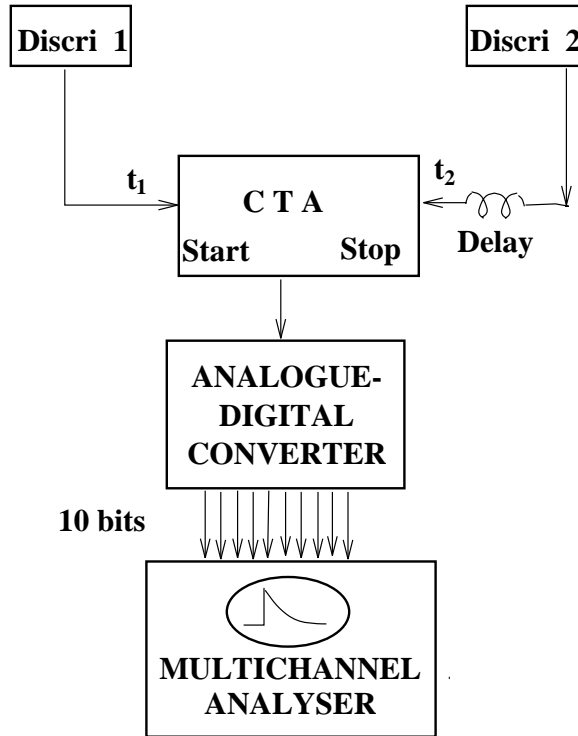


Figure VI-14: Coincidences by Time-Spectrum.

When $t_2 - t_1$ is between 0 and 100 ns, the numerical value for this time interval is obtained. The multichannel analyser constructs the corresponding histogram. The supplementary delay enables the channel corresponding to the simultaneous emission of ν_1 and ν_2 ($\tau = 0$) to be placed in the centre of the screen.

c) Orders of magnitude

[- 228 -]

Typical orders of magnitude (VI-6) are:

- True coincidences: $N_v = 200 \text{ s}^{-1}$

- Accidental coincidences: $\frac{dN_f}{d\tau} = 6.4 \times 10^9 \text{ s}^{-2}$

In each 0.1 ns channel, there may be a background of 0.64 accidental coincidences per second.

The true coincidences are distributed in a peak, followed by exponential decay of half-life 5 ns, corresponding to 50 channels. The channel with the highest score therefore has, in principle, 4 true coincidences per second. The contrast attained is of the order of 7.

Thus, at the end of 30 seconds of accumulation, 140 may be registered in the highest scoring channel, and 18 in the lower ones. The corresponding statistical variations are characterised by standard errors of 12 and 4 respectively, or 10% and 3% of the amplitude of the peak. The spectrum is thus clearly visible (Fig. VI-15-a). Moreover, it can be further improved by changing the scale to regroup the channels.

d) Centering of the spectrum

A supplementary delay can be introduced on the Stop pulses to make the simultaneous detections of ν_1 and ν_2 correspond, for example, to the channel situated in the centre of the histogram. It is as easy to construct the histogram associated with $\frac{dN_c}{d\tau}$ for negative delays as for positive ones. (Fig. VI-15)

[- 229 -]

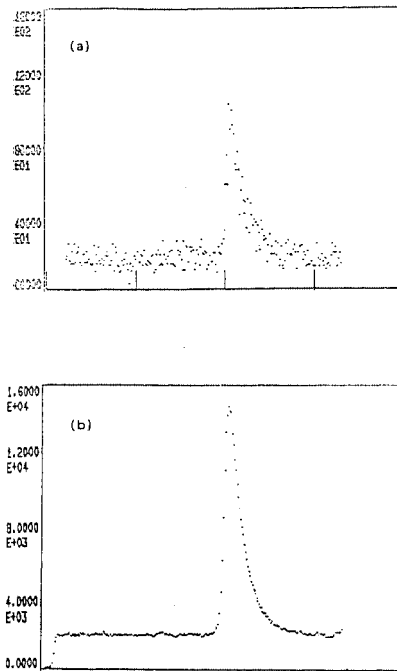


Figure VI-15: Time-Spectra for different accumulation times.

For this graphical representation, the ARIAM channels have been grouped in fours, so that there is 0.4 ns per channel.

(a) At tip of peak: 110 counts/channel.

(b) At tip of peak: 15000 counts/channel.

[- 230 -]

In practice, therefore, the pulses for photon ν_1 are applied to the Start input and those for ν_2 to the Stop, and the delay applied to the Stop adjusted so as to place the rising front of the peak for true coincidences in the centre of the screen. One is then sure that the channel is associated with the simultaneous emission of photons ν_1 and ν_2 , and there is no need to consider the details of the various delays that have accumulated along the two paths: the propagation times of the light, the

electronic transit times in the photomultipliers, the propagation times of the pulses in the electric cables, the delays of the discriminators, etc. . . .

By way of verification, we registered the time-spectrum constructed with a photodiode emitting light pulses of a few nanoseconds towards the two photomultipliers. We obtained a bell-shaped curve of 10 ns spread, which was centered on the rise front of the true coincidence peak.

Remark: *In the spectrum thus obtained, the delay has an algebraic significance. It enables the Start and Stop to be exchanged, giving a reversal of the curve.*

e) Linearity

The essential quality demanded of the C.T.A./C.A.N. ensemble is linearity of the relationship between the channel number and the Start-Stop time interval. If stochastically independent pulses are sent to the Start and Stop inputs, a white spectrum should be obtained, with no privileged delay.

This can be tested with two photomultipliers observing independent sources. Or one can use two generators of pulses with independent perturbations.

[- 231 -]

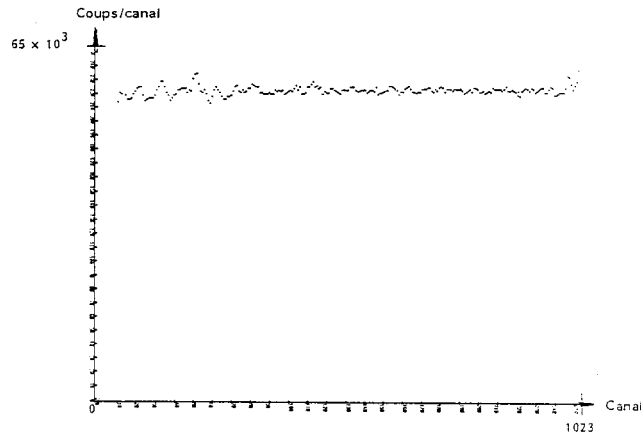


Figure VI-16: White time-spectrum of accidental coincidences, from which non-linearities can be estimated.

Fig. VI-16 shows a white spectrum obtained with singles counts similar to those used in the actual experiments (of the order of $8 \times 10^4 \text{ s}^{-1}$ for each path).

It is found that there are large non-linearities at the two extremities of the screen, this being an inherent feature of the Stop/Start circuits. By contrast, however, between channels numbers 300 and 950 the fluctuations – or *differential non-linearities* – are less than 2%. It is this zone that will be considered useful. The coincidence peak will be placed in the centre of the zone.

If the spectrum is smoothed by grouping adjacent channels, the fluctuations diminish. Smoothing over 10 ns (100 channels) leaves a residual fluctuation of less than 0.5% for the whole zone used. This figure characterises the *integral non-linearities* of the system. The remarkable regularity of the smoothed spectrum shows that evaluation of the base-

[- 232 -]

line of accidental coincidences can be done at any point within the useful zone.

Remark: *Many distinct white spectra showed the same fluctuations, which are thus reproducible. One can therefore, if necessary, correct for them by dividing the raw results by a reference white spectrum⁽¹¹⁰⁾.*

Remark: *If the probability of a Stop in the whole screen of the C.T.A. (10 ns) is not very small compared to 1, the end of the screen is less favoured: at counts of 10^5 Stops per second, the error reaches 1% at the end of the screen, and is not completely negligible. One can correct for this eventually in the calculations.*

f) Temporal resolution

The temporal resolution of the electronics used in registering the coincidence time spectra has been tested by sending synchronised electric pulses to the two discriminators for the Start and Stop paths, and verifying that the channel that is incremented is always the same. After two hours of stabilisation, the residual drift is less than 0.1 ns per hour, and the short-term variation is of the order of 0.1 ns (1 channel).

The time resolution is thus limited essentially by the photomultipliers (§ VI-C-2). The uncertainty translates, by convolution, into a gaussian of standard error 1 nanosecond, which reveals its presence in the rise time of the spectrum at $\tau = 0$ (Fig. VI-15).

g) Dead time

The complete treatment of a coincidence takes a variable time, mainly due to the analogue-digital conversion, and can take 20 μ s. During this time, the system is not able to deal with another coincidence.

In order to evaluate with precision the losses incurred in this way, for each detected coincidence we inhibited the C.T.A. for a fixed dead time of $25 \mu\text{s}$.

For 800 coincidences per second in the whole screen (200 true coincidences and 600 accidental ones), there will be a loss due to dead time of 2%. A correction can be made for this in the calculations.

There exists another cause of dead time: when the C.T.A. is activated by a Start and there is no Stop in the 100 ns window, the C.T.A. is not active again till 150 ns after the first Start. For 10^5 Starts per second, the correction for dead time is 1.5%; this must also be taken into account.

h) Conclusion

The registering of the time-spectrum is a privileged method for the study of coincidences. Graphical display of the spectrum gives precise information about the running of the experiment, and permits detection of anomalies.

[- 234 -]

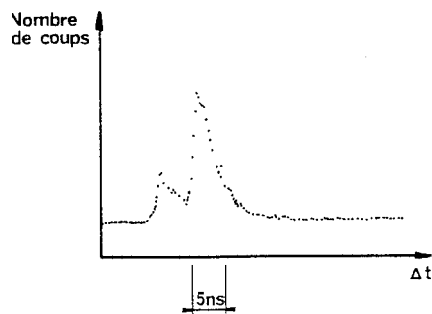


Figure VI-17: Abnormal time-spectrum. The secondary peak is due to a “parasitic” reflection from a filter.

By way of illustration, Fig. VI-17 shows a time-spectrum obtained in a preliminary phase of our experiments. The presence of a second peak reveals an anomaly that we have interpreted as due to reflection of photon ν_1 by the interference filter of path 2. This peak disappeared when we added, in front of the filters, coloured glass sheets that absorbed the unwanted wavelength (§ VI-B-3-b).

The inconvenience of the time-spectrum method is that the number of data items acquired is high (1024 for each spectrum), which necessitates the use of an on-line computer.

We used, in parallel, a much less demanding method: overlap-type coincidence circuits.

VI-C-4 Coincidences by overlap-type circuits

a) Principles

The overlap circuits are able to detect coincidences between N.I.M. pulses. These circuits, constructed around a logical ET circuit, give an output pulse if the two input pulses overlap for more than a duration u (Fig. VI-18).

A coincidence will be detected if:

$$t_2 \leq t_1 + l_1 - u \quad \text{and} \quad t_1 \leq t_2 + l_2 - u$$

that is to say

$$-l_2 + u \leq t_2 - t_1 \leq l_1 - u \quad (\text{VI} - 7)$$

[- 235 -]

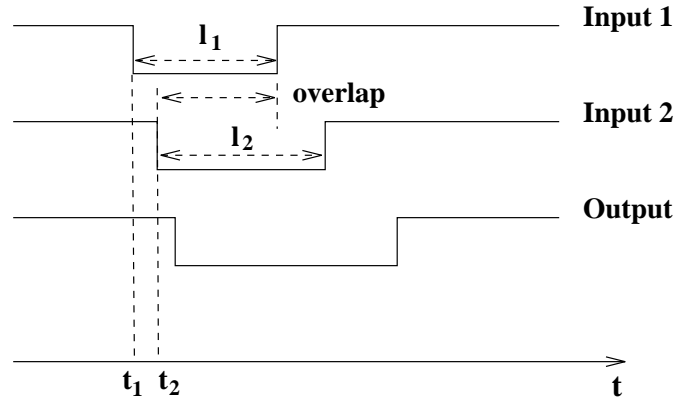


Figure VI-18: Coincidences by overlap-type circuits. The circuit produces an output pulse if the overlap (here $t_1 + l_1 - t_2$) exceeds a minimal duration, u .

The total number of coincidences detected is the integral of the time spectrum between $-l_2 + u$ and $l_1 - u$. The integration interval is termed the “coincidence window”, and has value:

$$w = l_1 + l_2 - 2u \quad (\text{VI} - 8)$$

The exact size of this coincidence window is important for interpreting the data.

[- 236 -]

The most natural way of determining it consists of applying to the two discriminator inputs pulses from the same generator, for which the relative delay is varied. The value of the delay $t_2 - t_1$ for which coincidences are obtained is then sought. This gives w directly, to about 2 ns (the precision of the variable delay line serves here).

We found windows w of the order of 20 ns, associated with input pulse lengths of $l_1 = l_2 = 16$ ns and minimum overlap of $u = 6$ ns.

A complementary estimate, that is in principle more precise, is obtained by applying independent random pulses to the two inputs. If the counts are N_1 and N_2 , a count of coincidences (accidental) should give:

$$N_f = wN_1N_2 \quad (\text{VI} - 9)$$

This method must be used with caution, as one must be sure that there is no correlation between the signals applied to the two routes. The best way to check this is to produce a simultaneous time spectrum, and to verify that it is flat, and that its average value, $dN_c/d\tau$, is in fact equal to the product N_1N_2 .

The coincidence window can then be estimated to within 0.1 ns. These measurements were made for each experiment, as the window depends on the coincidence and preceding circuits (through l_1 and l_2).

b) Adjustment of delays

The number of coincidences obtained in an experiment is the integral of the time spectrum $dN_c/d\tau$ taken over the coincidence window w . It is essential to place this window correctly with respect to the true coincidence peak.

[- 237 -]

To allow for the limits on time resolution (§ VI-C-2), the start of the window is placed at $\tau = -3$ ns, so that the end is at $\tau = -17$ ns. 97% of the true coincidences are then detected. If comparisons are needed with coincidence counts obtained with different circuits, such differences must be taken into account.

The exact positioning of the window is achieved by adjusting the delays on one route relative to the other. With the values above, the pulse associated with the second photon ν_2 must be advanced by 7 ns relative to that of the first photon ν_1 when the emissions are simultaneous (Fig. VI-19).

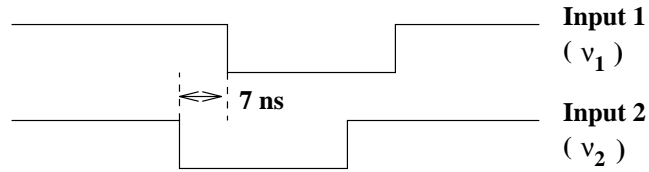


Figure VI-19: Pulses associated with two photons emitted simultaneously. At the input to the coincidence circuit the pulse associated with ν_2 is 7 ns in advance. In this way, coincidences are detected for delays between -3 ns and 17 ns.

The adjustment is easy to make, starting with a pulse generator producing pulses in both routes of the system in which the delay is chosen to give a signal in the $\tau = 0$ channel of the time spectrum; the lengths of the cables are then adjusted to give the situation shown in Fig. VI-19 at the coincidence circuit input.

c) Evaluation of accidental coincidences

[- 238 -]

The count N_c of coincidences obtained at the output of the centered overlap circuit is the sum of N_v true coincidences and N_f accidental ones. The problem is to evaluate N_f in order to subtract it from N_c .

Knowing the window w , N_f can be deduced from the singles counts N_1 and N_2 by the formula:

$$N_f = wN_1N_2 \quad (\text{VI-9})$$

The logic is not correct unless the source is rigorously stable. If there

are fluctuations, N_1 and N_2 are not independent and

$$N_f \geq w N_1 N_2 \quad (\text{VI-9}')$$

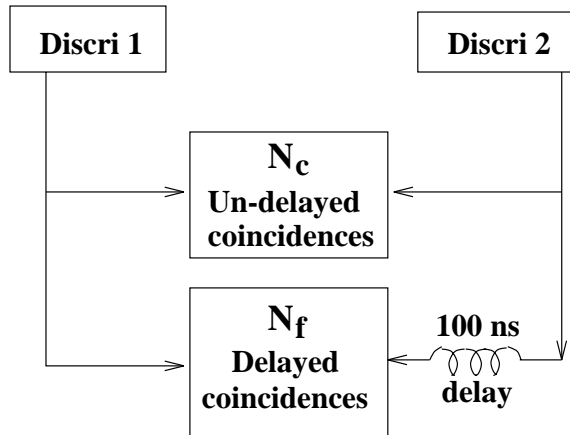


Figure VI-20: Measurement of coincidence counts using overlap circuits. The count of true coincidences is equal to $N_c - N_f$.

A more reliable method is to use a second circuit, with *delayed coincidences*. This circuit is parallel to the first (Fig. VI-20), but one of the routes is delayed by a time that is long in comparison with the peak of true coincidences (delay of 100 ns). This circuit can then register only accidental coincidences. If the correlation time of the source fluctuations is much longer than the delay, the accidental coincidence counts detected by the two circuits are equal, in proportion to their respective windows (which are in principle known with precision).

This method gives a ratio of signal to noise a little poorer than the time-spectrum method, as account must be taken of uncertainty in the

accidental coincidences. Nevertheless, the ratio of signal to noise is at worst divided by a factor of $\sqrt{2}$, and the conclusions of § V-1 relating to the optimal regime, and also to the orders of magnitude, remain essentially the same.

d) Verification of the method

[- 239 -]

A coincidence experiment was conducted in which the time-spectra of the counts N_c and N_f were registered simultaneously. After corrections for dead time, and taking into account the sizes of the coincidence windows, there should be equality of true coincidence counts by the two methods.

We checked this for each new experiment. The agreement obtained was always better than 1%.

e) Conclusion

The method using overlap circuits is convenient, as it is sufficient to record two numbers of each period of counting. Manual processing is then possible.

We think nevertheless that it should not be used as a standard method unless accompanied by a time-spectrum system. This gives permanent visual control of the absence of anomalies in the spectrum, and the results obtained by the two methods can be compared at any time.

VI-C-5 Processing of data

[- 240 -]

a) Counters

The singles counts, and the coincidences (provided by the overlap circuits) are accumulated by counters sensitive to N.I.M. pulses.

The assemblage of counters and the multichannel analyser are piloted by a clock that defines an accumulation period chosen between 1 s and 10^4 s. At the end of the period the data are recorded, and corrected for dead time according to the rule:

$$N_{true} = \frac{N_{counted}}{1 - TN_{counted}} \quad (\text{VI} - 10)$$

This correction is not valid unless there is a true dead time, that is to say, the counter is inhibited, after each detection, for a fixed time T , at the end of which it is again active. But events may often otherwise*: it can happen, for example, that a second pulse arrives during the “dead time” and prolongs the inhibition time.

In order to gain full control over dead time, we placed before the counter a circuit that shaped the pulse, so that we obtained the effect of true dead time, of fixed duration, which we chose to be a little longer than the longest dead time of the counter.

In the first experiments (Appendix VI), counters were used with dead times of 1 microsecond. For counts of $10^5 s^{-1}$, the correction was 10%.

[- 241 -]

Later we constructed a quadruple counter with dead time of 50 ns.

More recently, we have been equipped with a commercial N.I.M. module (BORER 341 A), comprising 12 counters with dead times of 20 ns. The

*This depends on the input circuitry of the counter.

correction (VI-10) then becomes completely negligible for singles counts that never exceed $5 \times 10^5 s^{-1}$.

b) Graphical display

In order to make adjustments or monitor the running of the experiment, the permanent display of the instantaneous mean values of certain counts is indispensable.

We adopted a very simple solution, consisting of sending the N.I.M. signals, suitably elongated, to a register that produced a mean by a mechanical inertia effect (integration time 0.1 s). The pulses have a constant amplitude (-0.8 V), and the signal obtained is proportional to the mean value, during the integration time, of the frequency of the pulses, so long as there is no overlap between pulses.

We adjusted the length of the pulses so as to obtain a mean signal of less than 20 mV (1/40th of the amplitude of the pulses). The cyclic ratio is then less than 1/40, and the error due to overlaps less than 2.5%.

Our two-channel analysers thus gave, throughout every experiment, the mean values of the two singles counts.

[- 242 -]

c) Transfer to computer

While we were limited to coincidences of two photomultipliers using overlap circuits, the volume of data acquired remained compatible with the use of pencil and paper (eventually, in a more recent version, the data were entered on a computer keyboard).

By contrast, it is almost impossible to note by hand the 1024 entries of the multichannel analyser! This operation was done only in excep-

tional circumstances (in the early experiments), in order to compare measurements by overlap circuit with those by time spectrum.

In the most elaborate version of our experiment (Chapter IX), the contents of the twelve counters, and of 4096 multichannel analyser channels, can be transferred when needed to the central mini-computer, which stores them on floppy disks. The final analysis of the data is performed with the same computer.

The transfer of a batch of data takes around ten seconds, during which the counts is halted. This transfer is done at the end of each accumulation period (typically 100 seconds or more).

Remark: *The complete automation of data acquisition presents a serious problem: the data is no longer examined in detail, as it would be when recorded by hand in a laboratory note book. We think that it is essential to retain control over the intermediate results. It is for this reason that we have multiplied the graphical controls, such as the permanent display of the time spectra, or the continuous trace of the mean counts.*

VI-C-6 Conclusion

[- 243 -]

Our electronics are characterised by the simultaneous use of two independent coincidence measurement systems, the results of which can be compared at any moment.

In general, we always measure quantities (for example, the coincidence windows for the overlap circuits) by independent methods.

The combined result of our efforts is the achievement of estimated precision and reproducibility of our measurements of better than 1%, which is of the same order as the stability of the source.

References

- [120] J. J. Samuéli, J. Pigneret and A. Sarazin, *Instrumentation électronique en physique nucléaire*, Masson, Paris (1968)

- [135] M. Duquesne and I. Tatischeff, Nucl. Instr. Methods **41**, (1966)

- [136] *Photomultiplicateurs*, Technical document RTC, Reference No. 5482-07 Paris (1981)